Environ Sci Pollut Res (2017) 24:17347–17357
DOI 10.1007/s11356-017-9329-2

RESEARCH ARTICLE

Green synthesis and characterization of gold and silver nanoparticles using *Mussaenda glabrata* leaf extract and their environmental applications to dye degradation

Sijo Francis[1] · **Siby Joseph**[2] · **Ebey P. Koshy**[1] · **Beena Mathew**[3]

Received: 24 March 2017 / Accepted: 19 May 2017 / Published online: 6 June 2017

Abstract Plant-derived nanomaterials opened a green approach in solving the current environment issues. Present study focused on rapid microwave-assisted synthesis and applications of gold and silver nanoparticles mediated by aqueous leaf extract of *Mussaenda glabrata*. The synthesized nanoparticles were characterized by UV-vis, FT-IR, powder XRD, energy-dispersive X-ray spectroscopy (EDX), transmission electron (TEM), and atomic force microscopic techniques (AFM). FCC crystal structure of both nanoparticles was confirmed by peaks corresponding to (111), (200), (220), and (311) planes in XRD spectra and bright circular spots in SAED pattern. IC_{50} values shown by gold and silver nanoparticles (44.1 ± 0.82 and 57.92 ± 1.33 μg/mL) reflected their high free radical scavenging potential. The synthesized gold and silver nanoparticles revealed their potency to inhibit pathogenic microorganisms *Bacillus pumilus*, *Staphylococcus aureus*, *Pseudomonas aeruginosa*, *Escherichia coli*, *Aspergillus niger*, and *Penicillium chrysogenum*. Anthropogenic pollutants rhodamine B and methyl orange were effectively degraded from aquatic environment and waste water sewages of dye industries using the prepared nanocatalysts. The catalytic capacities of the synthesized nanoparticles were also exploited in the reduction of 4-nitrophenol.

Keywords Green synthesis · *Mussaenda glabrata* · Metal nanoparticles · Catalysis · Rhodamine B · Methyl orange · 4-nitrophenol · Dye degradation · Water pollution

Highlights
- Gold and silver nanoparticles by easily mastered green microwave procedure.
- Triangular and spherical gold nanoparticles and quasi-spherical silver nanoparticles offer a new hope in water purification because of their excellent antimicrobial capacity.
- Antioxidant and antimicrobial efficacy increase their pharmaceutical value.
- Control of the environmental pollution utilizing the catalytic power of metal nanoparticles.
- Effective catalysts in the degradation of dyes.

Responsible editor: Suresh Pillai

Electronic supplementary material The online version of this article (doi:10.1007/s11356-017-9329-2) contains supplementary material, which is available to authorized users.

✉ Beena Mathew
beenamscs@gmail.com

Sijo Francis
srsijofrancis@gmail.com

Siby Joseph
sibyjoseph4@gmail.com

[1] Department of Chemistry, St. Joseph's College, Moolamattom, Idukki, Kerala 685591, India

[2] Department of Chemistry, St. George's College, Aruvithura, Kottayam, Kerala 686122, India

[3] School of Chemical Sciences, Mahatma Gandhi University, Kottayam, Kerala 686560, India

Introduction

Nanoregime size attributes awesome properties to noble metals which can be tailored according to our provision (Oemrawsingh et al. 2012). Designing and synthesizing novel products through less hazardous domain is a green chemistry perspective (Anastas and Kirchhoff 2002; Sheldon 2012). The inculcation of plant extracts in the metal nanoparticles synthesis is an environmentally benign approach and is a fast alternative to conventional chemical and physical methods (Ahmed et al. 2016a; Huo et al. 2017). Microwave-assisted synthesis is a green method, which eliminates the use of toxic

chemicals and reduces the preparation period (Joseph and Mathew 2015a). It is a nonclassic source of energy which improves quality and quantity of the product (Baghbanzadeh et al. 2011).

Plant extract supported gold and silver nanoparticles synthesis has been plentifully reported in the recently (Lallawmawma et al. 2015). The medicinal plant *Aerva lanata*, a rich reservoir of alkaloids and flavonoids, reduced $HAuCl_4$ and $AgNO_3$ to spherical gold and silver nanoparticles (Joseph and Mathew 2015b). Colloidal silver and gold nanoparticles were prepared at room temperature using aqueous and methanolic seed extract of *Dolichos biflorus* Linn (Basu et al. 2016). Gold and silver nanoparticles were prepared and stabilized using leaf extract of *Mentha piperita* which exhibited spherical geometry (MubarakAli et al. 2011). Phenolic hydroxyls present in the fruit extract of *Punica granatum* were used in the reduction of Ag^+ and Au^{3+} ions to polydispersed silver and gold nanoparticles (MeenaKumari and Philip 2015). Using aqueous root extract of *Glycyrrhiza uralensis*, spherical gold and silver nanoparticles were prepared by simple heating technique (Huo et al. 2017).

Green nanoparticles synthesis is simple and possesses innumerable applications (Mohanpuria et al. 2007; Abbasi et al. 2014). Biological applications of noble metal nanoparticles include their antimicrobial power (Ahmed et al. 2016a; Chung et al. 2016), in vitro antioxidant potential (Seralathan et al. 2014; Hong et al. 2016), anticoagulant capacity (Hamedi et al. 2017), and their cytotoxicity towards different cancerous cells (Das et al. 2013; Rathi Sre et al. 2015; Balashanmugam et al. 2016; Kim et al. 2016). Effectiveness of silver nanoparticles synthesized using plant extracts towards mosquito control was recently established (Benelli 2015).

The increased use of organic toxic chemicals contributed to water pollution as per the US Environmental Protection Agency (Ibrahim et al. 2016). Huge amounts of thousands of dyes and pigments were produced every year, 10–15% ejected out as effluents from industries (Subbaiah and Kim 2016). Environment polluting and human cancer-causing dyes were effectively removed from water bodies using the electron relay effects shown by the silver and gold nanocatalysts (Joseph and Mathew 2014a; Lim et al. 2016). Marine algae-reduced gold nanoparticles were catalytically employed in the reduction of various nitro compounds using $NaBH_4$ (Ramakrishna et al. 2016). Zero-valent metals in nanoscale help in environment remediation process (Li et al. 2016). Responsible usage of drinking water, strict control of water pollution, and novel technologies for waste water purification were inevitable for the survival of life in our planet.

Mussaenda glabrata (*M. glabrata*), a showy plant, belongs to Rubiaceae (coffee) family. It is found in wild forests in the Western Ghats of India. They have broad elliptical leaves, star-shaped deep red flowers, and beautiful white sepals which catch vision from a long distance. They flower almost all seasons throughout the year. *M. glabrata* is used to cure ulcers and asthma (Akter et al. 2013). The plant leaves were used as herbal shampoo, which improves hair growth and prevents dandruff. Recent reports of *Mussaenda* species unveiled that silver nanoparticles produced from $AgNO_3$ precursor using *Mussaenda erythrophylla* leaf extract advent a novel nanocatalyst for the decay of methyl orange (Varadavenkatesan et al. 2016).

In the present study, gold and silver nanoparticles were prepared using *M. glabrata* leaf extract from their respective metal salt precursors by microwave assistance. The synthesis under room temperature was also performed. We are able to demonstrate that the synthesized nanoparticles manifest excellent antioxidant and antimicrobial potentials which facilitate a broad envelop of biomedical functionalities embedded on them. The unquantifiable hazardous effects of environment polluting dyes rhodamine B and methyl orange were eliminated using the developed gold and silver nanoparticles. The catalytic ability of the nanoparticles to accelerate the reduction of 4-nitrophenol by the reductant $NaBH_4$ was also investigated.

Materials and methods

All chemicals used were of analytical grade. Chloroauric acid brought from Sigma-Aldrich. Silver nitrate, sodium borohydride, 4-nitrophenol, methyl orange, and rhodamine B were obtained from Merck India Ltd. All the reagents were applied without further purification.

Preparation of *M. glabrata* leaf extract

The fresh *M. glabrata* leaves were collected from wild realm in the month of August and were taxonomically identified (Fig. 1). Washed out all the dirt using double distilled water and 20 g of the sliced pieces was refluxed with 100 mL of double distilled water for 30 min at 70 °C. Then, filtration using Whatmann No.1 filter paper was done and the filtered extract was kept at 4 °C.

Room temperature synthesis of gold and silver nanoparticles

Using aqueous leaf extract of *M. glabrata*, gold and silver nanoparticles were prepared. A 1 mM solution of $HAuCl_4.3H_2O/AgNO_3$ was mixed well with the leaf extract (9:1) and kept it for 5 and 10 min, respectively, at room temperature (28 °C). Color change of the reaction mixtures was noted, and the spectroscopic confirmation for the formation of nanoparticles was done using electronic spectrophotometer.

Fig. 1 Photograph of the *Mussaenda glabrata* (*M. glabrata*) plant

Microwave-assisted synthesis of gold and silver nanoparticles

A house hold microwave oven (Sharp R-219T (W)) supplied the source of microwave energy. Gold/silver metal salt solution and plant extract were mixed in the ratio 9:1. Stirred the contents well and placed inside the oven for uniform microwave nurturing. After a period of 0.5 and 1 min, the nanoparticles formation was affirmed by UV-vis spectroscopy.

Purification of nanoparticles

The phytocomponents adhered on the microwave-synthesized gold and silver nanoparticles were removed by repeated centrifugation under 12,000 rpm in a refrigerated centrifuge. Decanted the supernatant liquid and redispersed the nanoparticles in double distilled water. The metal nanoparticles were dried in vacuum. The purified nanoparticles were used for analyses.

Characterization methods

UV-vis spectra were recorded using Shimadzu UV-2450 spectrophotometer. FT-IR spectra of the purified samples were done by Perkin Elmer Spectrum Two FT-IR spectrometer. The crystallographic information of the pure samples was documented by Bruker AXS D8 Advance X-ray diffractometer. Surface morphologic parameters were drawn from a JEOL JEM-2100 transmission electron microscope equipped with EDX attachment. AFM studies were conducted using WITec Alpha300 RA machine working in tapping mode.

Antioxidant potential assessment

The antioxidant potential of the leaf extract of *M. glabrata* and the nanoparticles derived from it were evaluated using DPPH assay. 1,1-diphenyl-2-picrylhydrazyl (DPPH) free radical is highly stabilized by the complete delocalization of an odd electron and it possesses a pink color with an absorption maximum at 517 nm in ethanol medium (Alam et al. 2013). When scavenged by hydrogen-donating substrates, color of the medium turned yellow. The decrease in absorbance at 517 nm is direct measure of free radical scavenging of a sample in terms of its hydrogen-donating ability (Chang et al. 2001). Different concentrations (12.5, 25, 50, 100, and 200 μg/mL) of antioxidant solutions were mixed with 0.1 mM DPPH solution in DMSO under dark condition and kept it at room temperature for 20 min under incubation. The absorbance at 517 nm for the samples was measured using UV-vis spectrophotometer. Plant extract and synthesized gold and silver nanoparticles were employed in the assessment process. Ascorbic acid functioned as the standard. Three milliliter of DPPH was taken as control. Inhibition (%) of the DPPH radical scavenging is calculated by the formula, Inhibition (%) = $(Abs_{Control} - Abs_{Sample})/Abs_{Control} \times 100$. The assessment was repeated in triplicate. IC_{50} values were estimated using Graph pad Prism software (Kharat and Mendhulkar 2016; Phull et al. 2016).

Antimicrobial study

Antimicrobial property of the set aside gold and silver nanoparticles was figured out by the well diffusion pathway using four bacterial and two fungal stains (Perugu et al. 2015; Rajan et al. 2015; Rathi Sre et al. 2015). Freshly prepared Petri plates with Muller Hinton Agar Medium were seeded with the bacteria namely, *Bacillus pumilus* (MTCC 1640), *Staphylococcus aureus* (MTCC 96), *Pseudomonas aeruginosa* (MTCC 424), *Escherichia coli* (MTCC 443). *Aspergillus niger* (MTCC 1344) and *Penicillium chrysogenum* (MTCC 5108) were spread on potato dextrose agar medium. All microorganisms were procured originally from Microbial Type Culture Collection, Institute of Microbial Technology, Chandigarh, India. Wells of 6 mm were bored using a well cutter and the nanoparticles were added to it. Standard drugs streptomycin and griseofulvin were used as positive control for antibacterial and antifungal studies. Sterilized water used as negative control. The diameter of the zone (mm) matured after 24 h incubation time around the well revealed the restriction capacity of the nanoparticles against the tested bacterial stains (Balouiri et al. 2016). After 1 week of incubation, the antifungal activity was measured as zone of inhibition in millimeter. All experiments were replicated and the mean and standard deviation of zone of inhibition were found out.

Statistical analysis

All the biological data were expressed as mean ± standard deviation, and the results were analyzed by one-way ANOVA followed by Tukey's post hoc analysis using Graph pad Prism software. A value of $p < 0.05$ was considered as statistically significant.

Catalytic capacity evaluation

Reduction of 4-nitrophenol

The potential of synthesized gold and silver nanoparticles to function as heterogeneous catalysts in aqueous media was exploited in the hydrogenation of 4-nitrophenol by $NaBH_4$ (Joseph and Mathew 2015b). A quartz cuvette containing 2 mL 4-nitrophenol (8×10^{-5} M), 0.5 mL of $NaBH_4$ (0.06 M), and 0.5 mL of the metal nanoparticles (0.02 mg/mL) were continuously monitored under UV-vis spectrophotometer at regular intervals. The rate mechanism was studied by noting the depletion in absorbance at 400 nm of the reaction aliquot.

Dye degradation reactions

The environment pollution caused by organic coloring pigments viz. rhodamine B and methyl orange can be removed by $NaBH_4$ using the synthesized gold and silver nanoparticles as catalysts. 2 mL rhodamine B (5×10^{-5} M) or methyl orange (8×10^{-5} M) and 0.5 mL (0.06 M) $NaBH_4$ were taken in a quartz cuvette of 3 mL capacity. To this, a fixed amount of gold/silver nanoparticles was added. The degradation of rhodamine B and methyl orange was monitored by time based UV-vis spectra. In order to investigate kinetics of the reaction, optical density at 553 and 464 nm for rhodamine B and methyl orange was measured, respectively, at different intervals (Joseph and Mathew 2015c).

Results and discussion

UV-vis spectral analysis

The genus *Mussaenda* is rich in alkaloids, steroids, flavonoids, and tannins. Most of the species had attractive antioxidant, antimicrobial, antipyretic, diuretic, and wound healing capacities. The species *Mussaenda* was used in traditional folk medicine in Chinese and Fijian culture (Vidyalakshmi et al. 2008). The UV-vis spectrum of *M. glabrata* leaf extract is shown in Fig. 2(a). The water-soluble components of *M. glabrata* leaves caused the reduction of trivalent gold and monovalent silver ions to the corresponding metal nanoparticles.

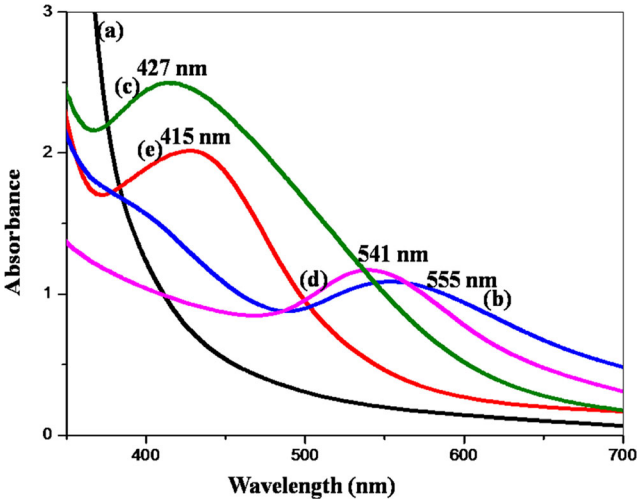

Fig. 2 UV-vis spectra of **a** *M. glabrata* leaf extract, **b** and **c** AuNP-*M. glabrata* and AgNP- *M. glabrata* prepared at room temperature, **d** and **e** AuNP- *M. glabrata* and AgNP- *M. glabrata* prepared under microwave irradiation

The preliminary observation for the formation of noble nanoparticles was the rapid color change of the reaction medium. The formation of gold nanoparticles is identified by the development of vivid ruby red color to the system. The onset of reddish brown shade indicated the generation of nascent silver nanoparticles. The gold and silver nanoparticles formation has been clearly rooted in their well-established surface plasmon resonance (SPR) absorptions in UV-vis spectra (Mittal et al. 2013). The SPR is the peculiar property of certain metal nanoparticles which arises due to the resonant oscillations of surface electrons with the frequencies of the electromagnetic radiations (Mulvaney 1996). The UV-vis spectrum of the gold and silver nanometals recorded after 5 and 10 min followed by the addition of *M. glabrata* extract to their metal salt solutions at room temperature (28°) is shown in Fig. 2(b and c). The SPR band corresponds to gold nanoparticles was 555 nm and that corresponds to silver was 427 nm.

Microwave irradiation of the similar reaction mixtures, for 0.5 and 1 min, has brought the gold and silver nanoparticles and the corresponding UV-vis spectra are shown in Fig. 2(d and e). The SPR peaks were found to be 541 nm and 415 nm, respectively, for gold and silver nanoparticles. It was well known that microwave synthetic route generates narrow-sized nanoparticles in a rapid manner compared to the other pathways (Joseph and Mathew 2014b). Formation of gold nanoparticles takes place more rapidly than silver nanoparticles due to the difference in reduction potential (Joseph and Mathew 2015b). The synthesized gold and silver nanoparticles were abbreviated as AuNP- *M. glabrata* and AgNP-*M. glabrata*. The photographs of *M. glabrata* leaf extract, AgNP- *M. glabrata*, and AuNP- *M. glabrata* are shown in Fig. 3.

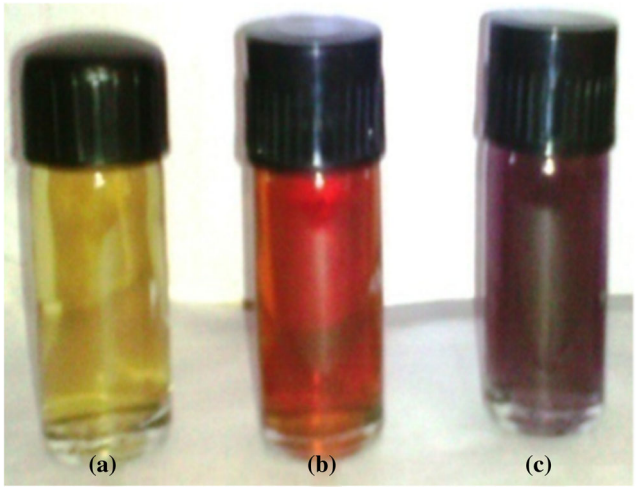

Fig. 3 Camera images of **a** aqueous *M. glabrata* leaf extract, **b** AgNP- *M. glabrata*, and **c** AuNP- *M. glabrata*

FT-IR spectra

The high potency of *M. glabrata* to perform the reduction process and to prevent the aggregation of the nanoparticles was due to the chemical components present in the aqueous leaf extract. The functional groups of the biomolecules were identified by Fourier transform infrared spectroscopy. FT-IR spectra of (a) *M. glabrata*, (b) AuNP- *M. glabrata*, and (c) AgNP- *M. glabrata* are exposed in Fig. 4. A broad peak at 3210 cm^{-1} of the leaf extract is due to N–H stretching of amines that is hydrogen bonded, and the peaks around 1732 and 1605 cm^{-1} are due to C = O stretching and C = C stretching of aromatic group, respectively. The sharp peaks centered at 1372 and 1015 cm^{-1} arise from –O–C– and –C–O–C– stretching modes. The aromatic –C–H bending vibrations showed peak at 824 cm^{-1}. The FT-IR spectra of gold and silver nanoparticles clearly coincide with that of *M. glabrata* leaf extract, proved its assistance in the formation and stabilization of nanoparticles.

X-ray powder diffractogram

The X-ray diffraction pattern of AuNP- *M. glabrata* exhibited fair peaks at 2θ positions 37.96°, 44.07°, 64.56°, and 77.59°. The X-ray powder diffractogram of the gold nanoparticles justified the crystalline nature with face centered cubic lattice. The diffraction of X-rays on AgNP- *M. glabrata* showed peaks at 37.83°, 43.99°, 64.26°, and 77.19° originated from (111), (200), (220), and (311) planes of face centered cubic lattice of nanosilver (Fig. 5). The most intense peak from AuNP- *M. glabrata* and AgNP- *M. glabrata* crystals was from (111) plane, revealed the preferred orientation of the crystals towards (111) plane (Kora et al. 2012; Sujitha and Kannan 2013).

TEM and EDX analyses

The electron micrographs investigated the surface features of the phytosynthesized nanoparticles. The morphological peculiarities of the microwave-generated gold nanoparticles like shape of the particles and allocations of the particle size were clearly visualized from the TEM images (Fig. 6). Spherical and triangular geometry of the nanogold is obviously depicted in the HR-TEM images (d). The gold nanoparticles have mean diameter of 10.59 nm. The elemental dispersive spectrum (g) confirmed the presence of gold.

The average size of the synthesized AgNP- *M. glabrata* is found to be 51.32 nm and has a notable spherical geometry (Fig. 7). The polydispersed and polycrystalline nature of the silver nanoparticles was also clear from the images (a–d). The selected area diffraction pattern (e) showed sharp diffraction spots in a circular arrangement arising from lattice reflections

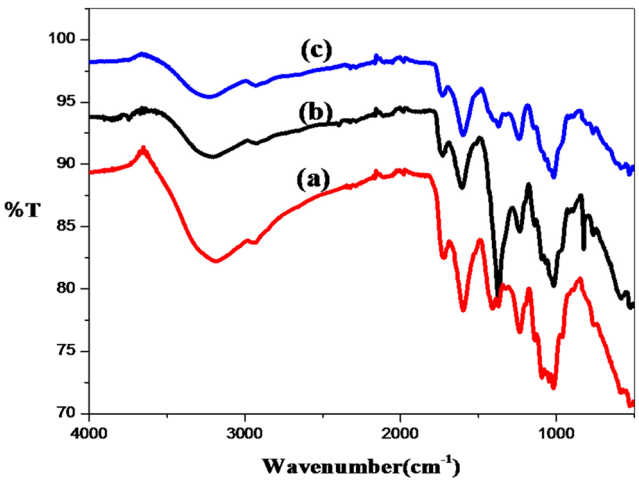

Fig. 4 FT-IR spectra of **a** *M. glabrata*, **b** AuNP- *M. glabrata*, and **c** AgNP- *M. glabrata*

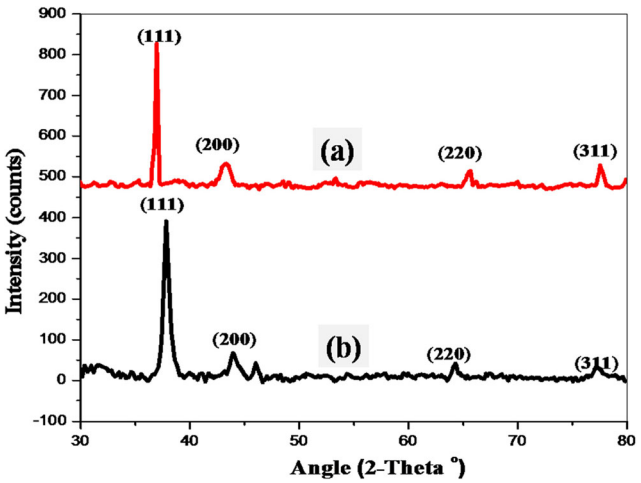

Fig. 5 X-ray diffraction spectra of **a** AuNP- *M. glabrata* and **b** AgNP- *M. glabrata*

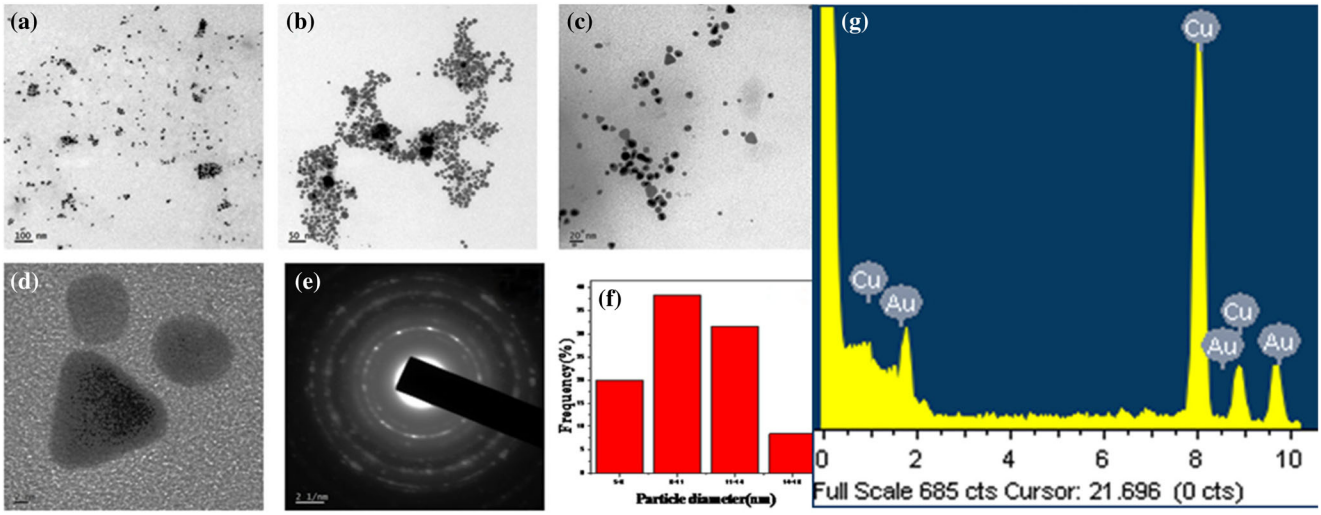

Fig. 6 **a**–**d** TEM images of AuNP- *M. glabrata* in diverse magnifications. **e** SAED patter. **f** The particle histogram. **g** EDX spectrum of AuNP- *M. glabrata*

from different planes of nanosilver. The EDX spectrum demonstrated the elemental presence silver (g).

Atomic force microscopy

The topographic information of materials was best studied by its response towards the atomic force microscope. This most versatile technology gave accurate two- and three-dimensional surface maps of the nanoparticles (Logeswari et al. 2015). Fig. S1 corresponds to AFM images of microwave-synthesized AgNP- *M. glabrata* and AuNP- *M. glabrata*.

The micrographic images revealed a nonuniform morphology arising from both the agglomerated and well-separated gold and silver nanoparticles (Jayaseelan et al. 2013). The topographic information of nanoparticles drawn by TEM is supplemented and supported by their atomic micrographs (Engelbrekt et al. 2009). The root mean square roughness obtained for AuNP- *M. glabrata* and AgNP- *M. glabrata* is 13.55 and 3.81 nm, respectively (Swamy et al. 2015).

Antioxidant capacity-DPPH method

The essential element oxygen creates highly reactive free radicals and resulted in various health disorders (Tong et al. 2015). Antioxidants were of natural or synthetic origin which counteracts the oxidation progress (Nimse and Pal 2015). Fresh fruits and vegetables were the best antioxidants, since they were rich in vitamin C, vitamin E, and β-carotene (Shashirekha et al. 2013; Moo-Huchin et al. 2015).

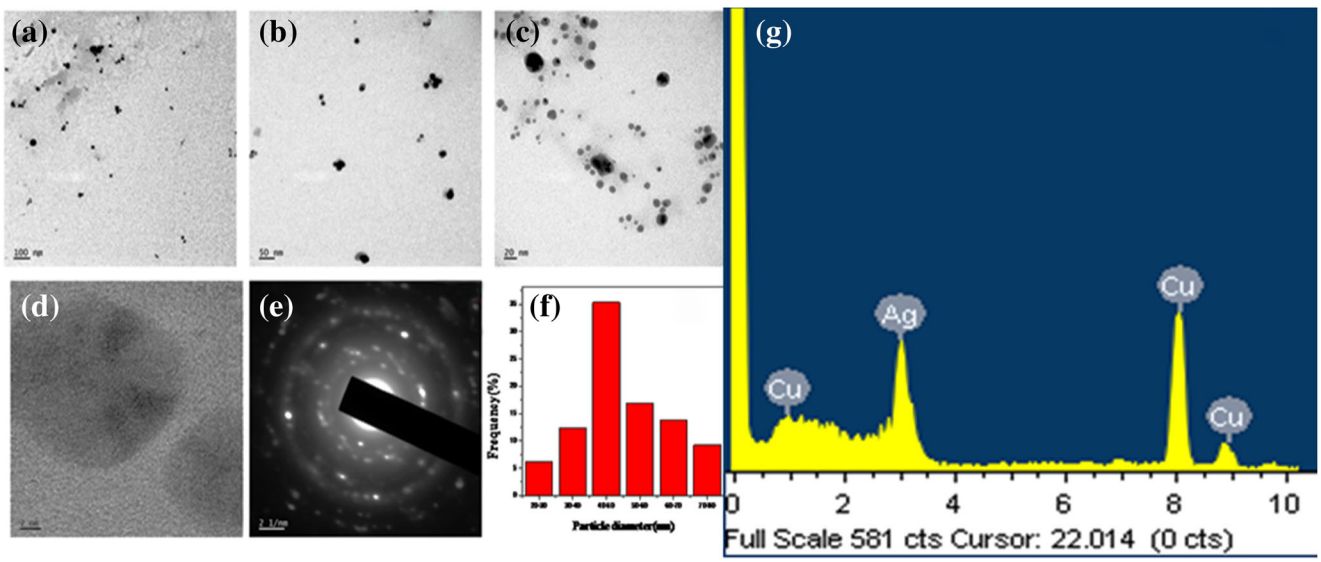

Fig. 7 **a**–**d** TEM images of AgNP- *M. glabrata* in different magnifications. **e** The SAED pattern. **f** The particle histogram. **g** EDX spectrum of AgNP- *M. glabrata*

Supplementation of antioxidants through diet or medication was a major strategy in medical science (Carlsen et al. 2010).

The potent antioxidant power of gold and silver nanoparticles (Fig. S2) showed a direct concentration dependency in the tested range (Kumar et al. 2016). Among silver and gold nanoparticles and plant extract, silver nanoparticles showed greater free radical scavenging potential than gold nanoparticles and plant extract. Silver and gold nanoparticles have greater capacity to undergo single electron transfer and to perform reduction of DPPH than the plant extract (Shahidi and Ambigaipalan 2015). IC_{50} values shown by AgNP-*M. glabrata*, AuNP- *M. glabrata*, and *M. glabrata* were 44.1 ± 0.82, 57.92 ± 1.33, and 169.13 ± 4.25 μg/mL, respectively, in comparison with 14.9 ± 0.33 μg/mL of standard, ascorbic acid. Biological activity expressed in terms of IC_{50} which reflected the concentration of the antioxidant needed to halve the initial concentration of DPPH. The antioxidant efficacy generally correlated to the oxidisable phenolic and flavonoid content of the plant extracts (Kalpanadevi and Mohan 2012). In vitro antioxidant potential of the prepared noble nanoparticles may offer remedy for oxidative stress.

Antimicrobial investigations

Substances which act against various functions of microorganisms were called antimicrobial agents. Plant-originated metal nanoparticles were proved to be potential antimicrobials (Balouiri et al. 2016) and are used to cure various infectious diseases (Rai et al. 2015). In vitro antimicrobial susceptibility of the microwave-synthesized silver and gold nanoparticles were tested by the agar well diffusion method. Fig. S3 exhibited the snapshots of different bacterial stains and fungal stains after an incubation period of 24 h and 7 days, respectively. The ability of nanoparticles to inhibit growth and action of microorganisms was expressed as the zone of inhibition (mm) formed around the well (Fig. S4).

The zone of inhibition certified that AgNP- *M. glabrata* and AuNP- *M. glabrata* were toxic to both gram positive and gram negative bacteria. The nanoparticles get diffused out of the well and interact with the microorganisms. The effected inhibition of microbial growth by the nanoparticles resulted in more or less circular zone. Many mechanisms were known for the antimicrobial action of metal nanoparticles. Nanoparticles may destroy cell membranes or prevent the functions of DNA mainly metabolism and replication (Prabhu and Poulose 2012; Hong et al. 2016). The metal nanoparticles showed different degree of inhibition towards the tested gram-positive and the gram-negative bacterial stains due to their difference in cell wall composition (Gurunathan 2014). The silver nanoparticles proved a better effectiveness than gold nanoparticles and are explained as the immobilization caused by agglomeration (Ramamurthy et al. 2013). The microwave-generated and *M. glabrata*-reduced gold and silver nanoparticles showed a moderate antifungal activity against the fungi *A. niger* and *P. chrysogenum* (Ahmed et al. 2016b). The bactericidal activity shown by nanoparticles mainly silver nanoparticles has an important use in water treatment (Hong et al. 2016).

Catalytic studies

Reduction of 4-nitrophenol to 4-aminophenol

An organic pollutant that generated by human involvement in the environment is 4-nitrophenol. It had an absorption maximum of 317 nm which was shifted to 400 nm by the introduction of $NaBH_4$ in aqueous medium resulting in the formation of 4-nitrophenolate ion (Rajan et al. 2015). Based on the reduction potential perspective, the conversion of 4-nitrophenol to 4-aminophenol using the reducing agent $NaBH_4$ was a thermodynamically allowed reaction (Otari et al. 2014). But it found that the required reduction was kinetically and practically forbidden even for a few couple of days by $NaBH_4$ alone (Gangula and Podila 2011).

The reduction of 4-nitrophenol was achieved by reducing agent $NaBH_4$ and utilizing the gold/silver nanocatalysts (Vilas et al. 2016). Adding 0.5 mL of AuNP- *M. glabrata* or AgNP-*M. glabrata* to the reaction cuvette containing 4-nitrophenol and $NaBH_4$, the reaction proceeds in a faster rate and reduction phenomena wonderfully ended up at 7 and 9 min (Fig. 8). The damping of absorbance at 400 nm indicated the progress of the reaction. The electron transfer from the BH_4^- to the electron accepter phenolic moiety was assisted and substantiated by the nanocatalysts. The gold and silver nanoparticles had ample surface area for the adsorption of the 4-nitrophenol and $NaBH_4$ and performed the electron relay process. The previously reported works forced to propose Langmuir-Hinshelwood model for this heterogeneous catalysis (Baruah et al. 2013). The reactions followed pseudo-first order kinetics with respect to 4-nitrophenol concentration, since the amount of $NaBH_4$ was surplus and thus practically remained constant all over the reaction. The pseudo-first-order rate constants with respect to 4-nitrophenol were also calculated from the kinetic plots following the rate equation $k = {}^{1}/_{t}\ln[A_0]/[A]$, where k is pseudo-first-order rate constant, $[A_0]$ is the initial concentration of 4-nitrophenol, and $[A]$ is concentration at time t (Yu et al. 2016; Manjari et al. 2017).

Dye degradation studies

Degradation of rhodamine B

Metal-chelating reagent rhodamine B is a dye used in paper, drug, and cosmetic industries. This dye pollutant causes an adverse effect on human eyes and skin. The taking away of

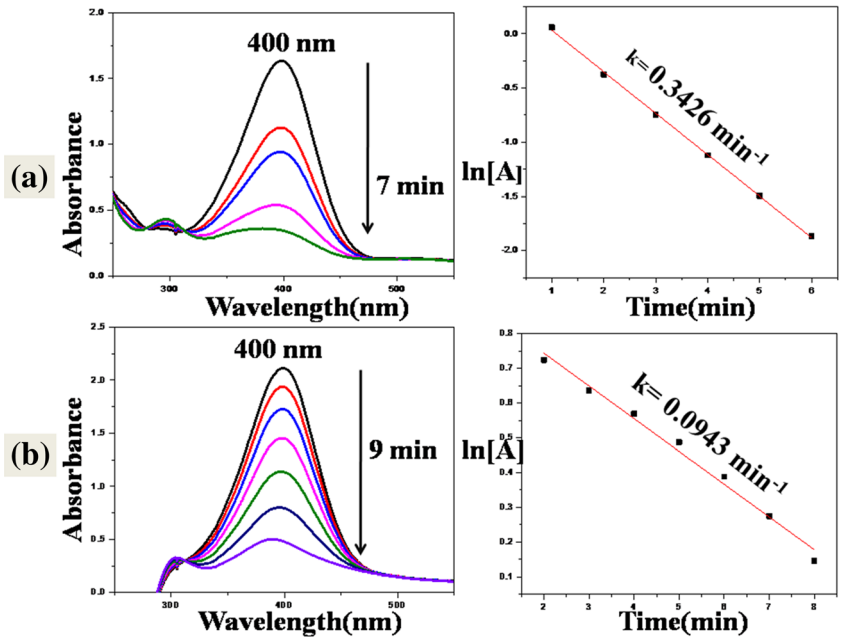

Fig. 8 Time dependent UV-vis spectra for the reduction of 4-nitrophenol by $NaBH_4$ catalyzed by **a** AuNP- *M. glabrata* (0.02 mg/mL) and **b** AgNP- *M. glabrata* (0.02 mg/mL)

this contaminating pigment from waste water is inadequate for healthy aquatic life (Wilhelm and Stephan 2007). In the absence of catalyst, the removal of rhodamine B takes place too slowly by $NaBH_4$ (Joseph and Mathew 2015c). AuNP- *M. glabrata* (5 μg/mL) and AgNP -*M. glabrata* (0.02 mg/mL) activated the complete removal of rhodamine B by 5 and 9 min. The deterioration reaction was monitored periodically by UV-vis absorption spectra (Fig. 9). The kinetic examination was conducted by listing the absorbance at 553 nm at different time gaps. The graph generated by plotting ln[A] verses time followed a linear behavior, and the reaction was found to pursue a pseudo-first-order with respect to rhodamine B concentration (Jeyapragasam and Kannan 2016). Catalytic rate constants for gold and silver nanoparticles were 0.7250 and 0.4464 min^{-1}, respectively.

The dye removal was happened through the shuttling of electrons between BH_4^- and the dye moiety at the surface of gold and silver nanocatalysts and rhodamine B get reduced to leuco rhodamine B (Paul et al. 2016). The surface of nanoparticles acted as heterogeneous catalyst following a Langmuir-Hinshelwood mechanism (Bastús et al. 2014; Bhargava et al. 2016).

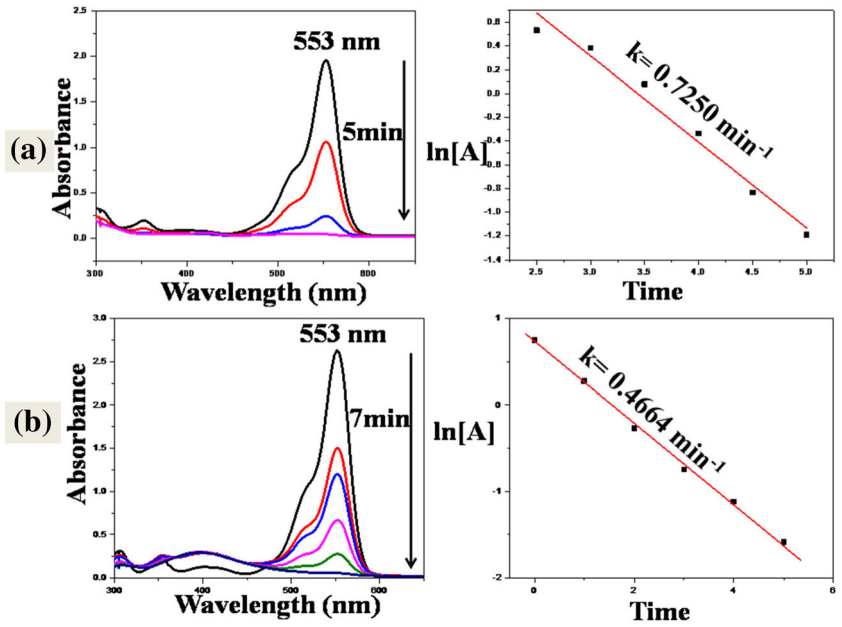

Fig. 9 Degradation of rhodamine B **a** in presence of AuNP- *M. glabrata* (5 μg/mL) and **b** in presence of AgNP- *M. glabrata* (0.02 mg/mL)

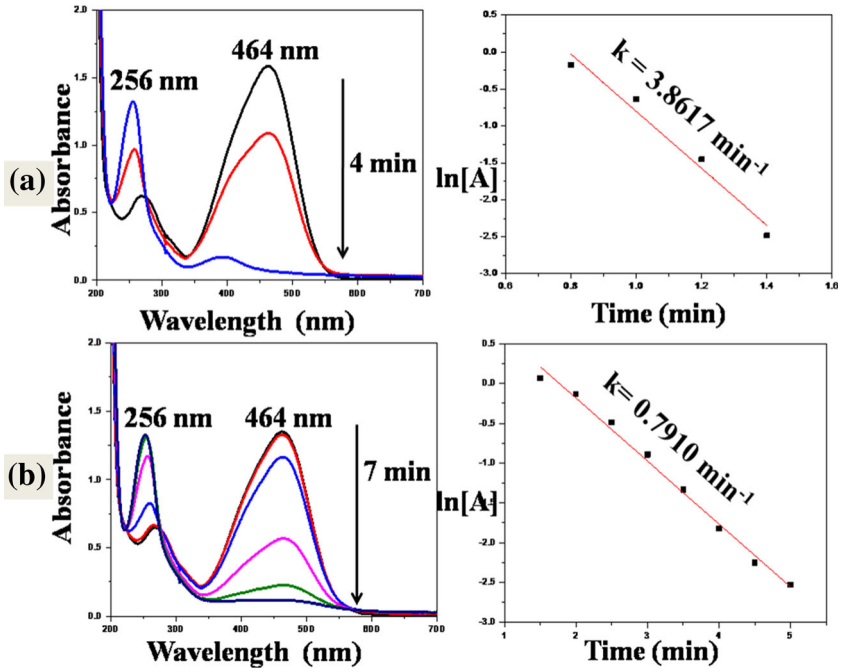

Fig. 10 Methyl orange degradation by $NaBH_4$ catalyzed by **a** AuNP- *M. glabrata* (0.01 mg/mL) and **b** AgNP- *M. glabrata* (0.01 mg/mL)

Degradation of methyl orange

Methyl orange is a toxic textile dye and possesses an appalling impact on aquatic kingdom. This azo dye has an absorption maximum of 464 nm in the UV-vis absorption spectra, due to N = N functional group. The reducing agent $NaBH_4$ alone was impotent in bringing the degradation of methyl orange (Vidhu and Philip 2014). The *glabrata*-reduced gold and silver nanocolloids executed the abolition of methyl orange within a period of 4 and 7 min, respectively, in a heterogeneous catalytic pathway (Fig. 10). Either the disappearance of peak at 464 nm or the appearance of peak at 256 nm due to the formation of product, hydrazine, indicates the removal of the methyl orange in the aqueous phase. The degradation of methyl orange passes through the transfer of an electron from donor to acceptor via the surface of the nanocatalysts (Varadavenkatesan et al. 2016). The catalytic degradation of methyl orange followed pseudo-first-order kinetics and can be beneficially exploited in water pollution government mission.

Conclusions

Gold and silver nanoparticles were synthesized by environmentally safe and facile route, namely, the microwave-assisted synthesis. The leaf extract of the wild medicinal plant *M. glabrata* acts as both reducing agent and antiagglomeration agent. The components of plant responsible for reduction and stabilization of gold and silver nanoparticles were identified by FT-IR spectroscopic analysis of the crude leaf extract. Colloidal metal nanoparticles were clearly characterized by UV-vis, powder X-ray diffraction, TEM, and AFM techniques. Gold and silver nanoparticles have excellent antioxidant characteristics, making them useful as therapeutic agents in future. Both nanoparticles were verified as good antimicrobial agents against different human disease-causing pathogens. The prepared gold and silver nanometals functioned as heterogeneous catalysts in different dye degradation perspectives. They offer new avenues for the perennial issues pertinent to waste water purification by degrading toxic contaminants.

Acknowledgements The financial assistance to Sijo Francis from University Grants Commission (under Faculty Development Programme), Government of India, is gratefully acknowledged.

Compliance with ethical standards

Conflict of interest The authors declare that they have no conflict of interest.

References

Abbasi E, Milani M, Fekri Aval S et al (2014) Silver nanoparticles: synthesis methods, bio-applications and properties. Crit Rev Microbiol: 1–8. doi:10.3109/1040841X.2014.912200

Ahmed S, Ahmad M, Swami BL, Ikram S (2016a) A review on plants extract mediated synthesis of silver nanoparticles for antimicrobial applications: a green expertise. J Adv Res 7:17–28. doi:10.1016/j.jare.2015.02.007

Akter R, Uddin SJ, Grice ID, Tiralongo E (2013) Cytotoxic activity screening of Bangladeshi medicinal plant extracts. J Nat Med 68: 246–252. doi:10.1007/s11418-013-0789-5

Alam MN, Bristi NJ, Rafiquzzaman M (2013) Review on in vivo and in vitro methods evaluation of antioxidant activity. Saudi Pharm J 21:143–152. doi:10.1016/j.jsps.2012.05.002

Anastas PT, Kirchhoff MM (2002) Origins, current status, and future challenges of green chemistry†. Acc Chem Res 35:686–694. doi:10.1021/ar010065m

Baghbanzadeh M, Carbone L, Cozzoli PD, Kappe CO (2011) Microwave-assisted synthesis of colloidal inorganic nanocrystals. Angew Chemie - Int Ed 50:11312–11359. doi:10.1002/anie.201101274

Balashanmugam P, Durai P, Balakumaran MD, Kalaichelvan PT (2016) Phytosynthesized gold nanoparticles from *C. roxburghii* DC. leaf and their toxic effects on normal and cancer cell lines. J Photochem Photobiol B Biol 165:163–173. doi:10.1016/j.jphotobiol.2016.10.013

Balouiri M, Sadiki M, Ibnsouda SK (2016) Methods for in vitro evaluating antimicrobial activity: a review. J Pharm Anal 6:71–79. doi:10.1016/j.jpha.2015.11.005

Baruah B, Gabriel GJ, Akbashev MJ, Booher ME (2013) Facile synthesis of silver nanoparticles stabilized by cationic polynorbornenes and their catalytic activity in 4-nitrophenol reduction. Langmuir 29:4225–4234

Bastús NG, Merkoçi F, Piella J, Puntes V (2014) Synthesis of highly monodisperse citrate-stabilized silver nanoparticles of up to 200 nm: kinetic control and catalytic properties. Chem Mater 26:2836–2846. doi:10.1021/cm500316k

Basu S, Maji P, Ganguly J (2016) Biosynthesis, characterisation and antimicrobial activity of silver and gold nanoparticles by *Dolichos biflorus* Linn seed extract. J Exp Nanosci 11:660–668. doi:10.1080/17458080.2015.1112042

Benelli G (2015) Plant-mediated biosynthesis of nanoparticles as an emerging tool against mosquitoes of medical and veterinary importance: a review. Parasitol Res 115:23–34. doi:10.1007/s00436-015-4800-9

Bhargava A, Jain N, Khan MA et al (2016) Utilizing metal tolerance potential of soil fungus for efficient synthesis of gold nanoparticles with superior catalytic activity for degradation of rhodamine B. J Environ Manag 183:22–32. doi:10.1016/j.jenvman.2016.08.021

Carlsen MH, Halvorsen BL, Holte K et al (2010) The total antioxidant content of more than 3100 foods, beverages, spices, herbs and supplements used worldwide. Nutr J 9:3. doi:10.1186/1475-2891-9-3

Chang S-T, Wu J-H, Wang S-Y et al (2001) Antioxidant activity of extracts from *Acacia confusa* bark and heartwood. J Agric Food Chem 49:3420–3424. doi:10.1021/jf0100907

Chung I-M, Park I, Seung-Hyun K et al (2016) Plant-mediated synthesis of silver nanoparticles: their characteristic properties and therapeutic applications. Nanoscale Res Lett 11:40. doi:10.1186/s11671-016-1257-4

Das S, Das J, Samadder A et al (2013) Biosynthesized silver nanoparticles by ethanolic extracts of *Phytolacca decandra*, *Gelsemium sempervirens*, *Hydrastis canadensis* and *Thuja occidentalis* induce differential cytotoxicity through G2 / M arrest in A375 cells. Colloids Surfaces B Biointerfaces 101:325–336. doi:10.1016/j.colsurfb.2012.07.008

Engelbrekt C, Sørensen KH, Zhang J et al (2009) Green synthesis of gold nanoparticles with starch–glucose and application in bioelectrochemistry. J Mater Chem 19:7839. doi:10.1039/b911111e

Gangula A, Podila RMR et al (2011) Catalytic reduction of 4-nitrophenol using biogenic gold and silver nanoparticles derived from Breynia rhamnoides. Langmuir 27:15268–15274. doi:10.1021/la2034559

Gurunathan S (2014) Rapid biological synthesis of silver nanoparticles and their enhanced antibacterial effects against Escherichia fergusonii and Streptococcus mutans. Arab J Chem. doi:10.1016/j.arabjc.2014.11.014

Hamedi S, Shojaosadati SA, Mohammadi A (2017) Evaluation of the catalytic, antibacterial and anti-biofilm activities of the *Convolvulus arvensis* extract functionalized silver nanoparticles. J Photochem Photobiol B Biol 167:36–44. doi:10.1016/j.jphotobiol.2016.12.025

Hong X, Wen J, Xiong X, Hu Y (2016) Shape effect on the antibacterial activity of silver nanoparticles synthesized via a microwave-assisted method. Environ Sci Pollut Res 23:4489–4497. doi:10.1007/s11356-015-5668-z

Huo Y, Singh P, Kim YJ et al (2017) Biological synthesis of gold and silver chloride nanoparticles by Glycyrrhiza uralensis and in vitro applications. Artif Cells, Nanomedicine, Biotechnol 4:1–13. doi:10.1080/21691401.2017.1307213

Ibrahim RK, Hayyan M, AlSaadi MA et al (2016) Environmental application of nanotechnology: air, soil, and water. Environ Sci Pollut Res 23:13754–13788. doi:10.1007/s11356-016-6457-z

Jayaseelan C, Ramkumar R, Rahuman AA, Perumal P (2013) Green synthesis of gold nanoparticles using seed aqueous extract of *Abelmoschus esculentus* and its antifungal activity. Ind Crop Prod 45:423–429. doi:10.1016/j.indcrop.2012.12.019

Jeyapragasam T, Kannan RS (2016) Microwave assisted green synthesis of silver nanorods as catalysts for rhodamine B degradation. Russ J Phys Chem A 90:1334–1337. doi:10.1134/S003602441607030X

Joseph S, Mathew B (2014a) Microwave-assisted facile synthesis of silver nanoparticles in aqueous medium and investigation of their catalytic and antibacterial activities. J Mol Liq 197:346–352. doi:10.1016/j.molliq.2014.06.008

Joseph S, Mathew B (2014b) Microwave assisted biosynthesis of silver nanoparticles using the rhizome extract of *Alpinia galanga* and evaluation of their catalytic and antimicrobial activities. J Nanoparticles 2014:9. doi:10.1155/2014/967802

Joseph S, Mathew B (2015a) Microwave-assisted green synthesis of silver nanoparticles and the study on catalytic activity in the degradation of dyes. J Mol Liq 204:184–191. doi:10.1016/j.molliq.2015.01.027

Joseph S, Mathew B (2015b) Microwave assisted facile green synthesis of silver and gold nanocatalysts using the leaf extract of *Aerva lanata*. Spectrochim Acta - Part A Mol Biomol Spectrosc 136:1371–1379. doi:10.1016/j.saa.2014.10.023

Joseph S, Mathew B (2015c) Facile synthesis of silver nanoparticles and their application in dye degradation. Mater Sci Eng B 195:90–97. doi:10.1016/j.mseb.2015.02.007

Kalpanadevi V, Mohan VR (2012) In vitro antioxidant studies of Begonia malabarica Lam. and Begonia floccifera Bedd. Asian Pac J Trop Biomed 2:S1572–S1577. doi:10.1016/S2221-1691(12)60455-9

Kharat SN, Mendhulkar VD (2016) Synthesis, characterization and studies on antioxidant activity of silver nanoparticles using *Elephantopus scaber* leaf extract. Mater Sci Eng C 62:719–724. doi:10.1016/j.msec.2016.02.024

Kim Y-J, Wang C, Mathiyalagan R et al (2016) Rapid green synthesis of silver and gold nanoparticles using Dendropanax morbifera leaf extract and their anticancer activities. Int J Nanomedicine 11:3691–3701. doi:10.2147/IJN.S97181

Kora AJ, Sashidhar RB, Arunachalam J (2012) Aqueous extract of gum olibanum (*Boswellia serrata*): a reductant and stabilizer for the biosynthesis of antibacterial silver nanoparticles. Process Biochem 47:1516–1520. doi:10.1016/j.procbio.2012.06.004

Kumar B, Smita K, Cumbal L et al (2016) One pot phytosynthesis of gold nanoparticles using *Genipa americana* fruit extract and its biological applications. Mater Sci Eng C 62:725–731. doi:10.1016/j.msec.2016.02.029

Lallawmawma H, Sathishkumar G, Sarathbabu S et al (2015) Synthesis of silver and gold nanoparticles using Jasminum nervosum leaf extract and its larvicidal activity against filarial and arboviral vector *Culex quinquefasciatus* Say (Diptera: Culicidae). Environ Sci Pollut Res 22:17753–17768. doi:10.1007/s11356-015-5001-x

Li L, Hu J, Shi X et al (2016) Nanoscale zero-valent metals: a review of synthesis, characterization, and applications to environmental remediation. Environ Sci Pollut Res 23:17880–17900. doi:10.1007/s11356-016-6626-0

Lim SH, Ahn E-Y, Park Y (2016) Green synthesis and catalytic activity of gold nanoparticles synthesized by Artemisia capillaris water extract. Nanoscale Res Lett 11:474. doi:10.1186/s11671-016-1694-0

Logeswari P, Silambarasan S, Abraham J (2015) Synthesis of silver nanoparticles using plants extract and analysis of their antimicrobial property. J Saudi Chem Soc 19:311–317. doi:10.1016/j.jscs.2012.04.007

Manjari G, Saran S, Arun T et al (2017) Facile Aglaia elaeagnoidea mediated synthesis of silver and gold nanoparticles: antioxidant and catalysis properties. J Clust Sci. doi:10.1007/s10876-017-1199-8

MeenaKumari M, Philip D (2015) Degradation of environment pollutant dyes using phytosynthesized metal nanocatalysts. Spectrochim Acta - Part A Mol Biomol Spectrosc 135:632–638. doi:10.1016/j.saa.2014.07.037

Mittal AK, Chisti Y, Banerjee UC (2013) Synthesis of metallic nanoparticles using plant extracts. Biotechnol Adv 31:346–356. doi:10.1016/j.biotechadv.2013.01.003

Mohanpuria P, Rana NK, Yadav SK (2007) Biosynthesis of nanoparticles: technological concepts and future applications. J Nanopart Res 10:507–517. doi:10.1007/s11051-007-9275-x

Moo-Huchin VM, Moo-Huchin MI, Estrada-León RJ et al (2015) Antioxidant compounds, antioxidant activity and phenolic content in peel from three tropical fruits from Yucatan, Mexico. Food Chem 166:17–22. doi:10.1016/j.foodchem.2014.05.127

MubarakAli D, Thajuddin N, Jeganathan K, Gunasekaran M (2011) Plant extract mediated synthesis of silver and gold nanoparticles and its antibacterial activity against clinically isolated pathogens. Colloids Surfaces B Biointerfaces 85:360–365. doi:10.1016/j.colsurfb.2011.03.009

Mulvaney P (1996) Surface plasmon spectroscopy of nanosized metal particles. Langmuir 12:788–800. doi:10.1021/la9502711

Nimse SB, Pal D (2015) Free radicals, natural antioxidants, and their reaction mechanisms. RSC Adv 5:27986–28006. doi:10.1039/c4ra13315c

Oemrawsingh SSR, Markešević N, Gwinn EG et al (2012) Spectral properties of individual DNA-hosted silver nanoclusters at low temperatures. J Phys Chem C 116:25568–25575. doi:10.1021/jp307848t

Otari S, Patil RM, Nadaf NH et al (2014) Green synthesis of silver nanoparticles by microorganism using organic pollutant: its antimicrobial and catalytic application. Environ Sci Pollut Res 21:1503–1513. doi:10.1007/s11356-013-1764-0

Paul B, Bhuyan B, Purkayastha DD, Dhar SS (2016) Photocatalytic and antibacterial activities of gold and silver nanoparticles synthesized using biomass of *Parkia roxburghii* leaf. J Photochem Photobiol B Biol 154:1–7. doi:10.1016/j.jphotobiol.2015.11.004

Perugu S, Nagati V, Bhanoori M (2015) Green synthesis of silver nanoparticles using leaf extract of medicinally potent plant Saraca indica: a novel study. Appl Nanosci 6:747–753. doi:10.1007/s13204-015-0486-7

Phull A-R, Abbas Q, Ali A et al (2016) Antioxidant, cytotoxic and antimicrobial activities of green synthesized silver nanoparticles from crude extract of Bergenia ciliata. Futur J Pharm Sci 2:31–36. doi:10.1016/j.fjps.2016.03.001

Prabhu S, Poulose EK (2012) Silver nanoparticles: mechanism of antimicrobial action, synthesis, medical applications, and toxicity effects. Int Nano Lett 2:32. doi:10.1186/2228-5326-2-32

Rai M, Ingle AP, Birla S, et al (2015) Strategic role of selected noble metal nanoparticles in medicine. Crit Rev Microbiol 1–24. doi: 10.3109/1040841X.2015.1018131

Rajan A, Vilas V, Philip D (2015) Studies on catalytic, antioxidant, antibacterial and anticancer activities of biogenic gold nanoparticles. J Mol Liq 212:331–339. doi:10.1016/j.molliq.2015.09.013

Ramakrishna M, Rajesh Babu D, Gengan RM et al (2016) Green synthesis of gold nanoparticles using marine algae and evaluation of their catalytic activity. J Nanostructure Chem 6:1–13. doi:10.1007/s40097-015-0173-y

Ramamurthy C, Padma M, Mariya Samadanam ID et al (2013) The extra cellular synthesis of gold and silver nanoparticles and their free radical scavenging and antibacterial properties. Colloids Surfaces B Biointerfaces 102:808–815. doi:10.1016/j.colsurfb.2012.09.025

Rathi Sre PR, Reka M, Poovazhagi R et al (2015) Antibacterial and cytotoxic effect of biologically synthesized silver nanoparticles using aqueous root extract of *Erythrina indica* lam. Spectrochim Acta - Part A Mol Biomol Spectrosc 135:1137–1144. doi:10.1016/j.saa.2014.08.019

Seralathan J, Stevenson P, Subramaniam S et al (2014) Spectroscopy investigation on chemo-catalytic, free radical scavenging and bactericidal properties of biogenic silver nanoparticles synthesized using Salicornia brachiata aqueous extract. Spectrochim Acta - Part A Mol Biomol Spectrosc 118:349–355. doi:10.1016/j.saa.2013.08.114

Shahidi F, Ambigaipalan P (2015) Phenolics and polyphenolics in foods, beverages and spices: antioxidant activity and health effects—a review. J Funct Foods 18:820–897. doi:10.1016/j.jff.2015.06.018

Shashirekha MN, Mallikarjuna SE, Rajarathnam S (2013) Status of bioactive compounds in foods, with focus on fruits and vegetables. Crit Rev Food Sci Nutr 55:1324–1339. doi:10.1080/10408398.2012.692736

Sheldon RA (2012) Fundamentals of green chemistry: efficiency in reaction design. Chem Soc Rev 41:1437–1451. doi:10.1039/c1cs15219j

Subbaiah MV, Kim D-S (2016) Adsorption of methyl orange from aqueous solution by aminated pumpkin seed powder: kinetics, isotherms, and thermodynamic studies. Ecotoxicol Environ Saf 128:109–117. doi:10.1016/j.ecoenv.2016.02.016

Sujitha MV, Kannan S (2013) Green synthesis of gold nanoparticles using citrus fruits (*Citrus limon*, *Citrus reticulata* and *Citrus sinensis*) aqueous extract and its characterization. Spectrochim Acta - Part A Mol Biomol Spectrosc 102:15–23. doi:10.1016/j.saa.2012.09.042

Swamy MK, Akhtar MS, Mohanty SK, Sinniah UR (2015) Synthesis and characterization of silver nanoparticles using fruit extract of Momordica cymbalaria and assessment of their in vitro antimicrobial, antioxidant and cytotoxicity activities. Spectrochim Acta Part A Mol Biomol Spectrosc 151:939–944. doi:10.1016/j.saa.2015.07.009

Tong L, Chuang C-C, Wu S, Zuo L (2015) Reactive oxygen species in redox cancer therapy. Cancer Lett 367:18–25. doi:10.1016/j.canlet.2015.07.008

Varadavenkatesan T, Selvaraj R, Vinayagam R (2016) Phyto-synthesis of silver nanoparticles from Mussaenda erythrophylla leaf extract and their application in catalytic degradation of methyl orange dye. J Mol Liq 221:1063–1070. doi:10.1016/j.molliq.2016.06.064

Vidhu VK, Philip D (2014) Catalytic degradation of organic dyes using biosynthesized silver nanoparticles. Micron 56:54–62. doi:10.1016/j.micron.2013.10.006

Vidyalakshmi KS, Vasanthi HR, Rajamanickam G V (2008) Ethnobotany, phytochemistry and pharmacology of *Mussaenda* species (Rubiaceae). Ethnobot Leafl 12:469–475.

Vilas V, Philip D, Mathew J (2016) Essential oil mediated synthesis of silver nanocrystals for environmental, anti-microbial and antioxidant applications. Mater Sci Eng C 61:429–436. doi:10.1016/j.msec.2015.12.083

Wilhelm P, Stephan D (2007) Photodegradation of rhodamine B in aqueous solution via SiO2@TiO2 nano-spheres. J Photochem Photobiol A Chem 185:19–25. doi:10.1016/j.jphotochem.2006.05.003

Yu J, Xu D, Guan HN et al (2016) Facile one-step green synthesis of gold nanoparticles using *Citrus maxima* aqueous extracts and its catalytic activity. Mater Lett 166:110–112. doi:10.1016/j.matlet.2015.12.031